Aluminium in the North Atlantic Ocean and the Labrador Sea (GEOTRACES GA01 section): roles of continental inputs and biogenic particle removal

Jan-Lukas Menzel Barraqueta[1], Christian Schlosser[1], Hélène Planquette[2], Arthur Gourain[2,3], Marie Cheize[2], Julia Boutorh[2], Rachel Shelley[2,4,5], Leonardo Pereira Contreira[6], Martha Gledhill[1], Mark J. Hopwood[1], Pascale Lherminier[7], Geraldine Sarthou[2], Eric P. Achterberg[1]

[1] GEOMAR, Helmholtz Centre for Ocean Research Kiel, Germany
[2] LEMAR, UMR 6539, Plouzané, France
[3] Earth, Ocean and Ecological Sciences-School of Environmental Sciences, University of Liverpool, UK
[4] Earth, Ocean and Atmospheric Science, Florida State University, Tallahassee, Florida, USA
[5] Geography, Earth and Environmental Sciences, University of Plymouth, UK
[6] Universidade Federal do Rio Grande-FURG, Rio Grande, Brazil
[7] Ifremer, Laboratoire d'Océanographie Physique et Spatiale (LOPS), IUEM, Plouzané, France

Correspondence to: Jan-Lukas Menzel Barraqueta (jmenzel@geomar.de)

Abstract

The distribution of dissolved aluminium (dAl) in the water column of the North Atlantic and Labrador Sea was studied along GEOTRACES section GA01 to unravel the sources and sinks of this element. Surface water dAl concentrations were low (median of 2.5 nM) due to low aerosol deposition and removal by phytoplankton. However, surface water dAl concentrations were enhanced on the Iberian and Greenland shelves (up to 30.9 nM) due to continental inputs (rivers, glacial flour and ice melt). A negative correlation was observed between dAl in surface waters and primary production, phytoplankton community structure and biogenic opal production. The abundance of diatoms exerted a significant ($p<0.01$) control on the surface particulate Al (pAl) to dAl ratios by decreasing dAl levels and increasing pAl levels. Dissolved Al concentrations generally increased with depth and correlated strongly with silicate ($R^2>0.76$) west of the Iberian Basin, suggesting net release of dAl at depth during remineralization of sinking biogenic opal containing particles. Enrichment of dAl at near-bottom depths was observed due to resuspension of sediments near the sediment-water interface. The highest dAl (up to 38.7 nM) concentrations were observed in Mediterranean Overflow Waters which act as a major source of dAl to mid depth waters of the eastern North Atlantic. This study clearly shows that the vertical and lateral distribution of dAl in the North Atlantic differs when compared to other regions of the North Atlantic and global ocean due to the large spatial differences both in the main source of Al, atmospheric deposition, and the main sink for Al, particle scavenging, between different oceanic regions.

1 Introduction

Aluminium (Al) in the oceans has been used as a tracer for mineral dust deposition (Han et al., 2008; Measures and Vink, 2000; Measures and Brown, 1996) and water masses (Measures and Edmond, 1990). Aluminium is the third most abundant element in the Earth´s crust (Rudnick and Gao, 2003), but

5 concentrations of dissolved Al (dAl; filtered through 0.4 or 0.2 µm pore size filters) in the world´s ocean are limited to nanomolar to low micromolar levels. In seawater, Al undergoes rapid hydrolysis resulting in the formation of species such as $Al(OH)_3$ and $Al(OH)_4^-$ (Orians and Bruland, 1986, 1985), which are insoluble (Roberson and Hem, 1969) and particle reactive (Orians and Bruland, 1985), especially in association with silicon-rich particles (Moran and Moore, 1988).

10 A major source of Al to the surface ocean is dry atmospheric deposition of terrigenous material (Kramer et al., 2004; Measures et al., 2005; Orians and Bruland, 1986) which can be carried thousands of kilometres in the atmosphere before deposition in the ocean (Duce et al., 1991; Prospero and Carlson, 1972). Wet atmospheric deposition (rain, fog and snow) also plays an important role in supplying Al to the North Atlantic (Schlosser et al., 2014; Shelley et al., 2017) and the global ocean (Guerzoni et al.,

15 1997; Vink and Measures, 2001). Glacial run off has been reported as a pronounced source for Arctic and Antarctic surface waters (Brown et al., 2010; Schlosser et al., 2017), but its importance beyond the immediate source regions has not yet been established. Fluvial inputs were historically considered a dominant source of Al to the surface oceans (Stoffyn and Mackenzie, 1982), but Al removal during estuarine scavenging processes appears to strongly reduce the riverine Al outflow (Hydes, 1989).

20 Sediment resuspension processes at ocean margins with strong boundary currents (Jeandel et al., 2011) and in benthic nepheloid layers (BNLs) (Hesse et al., 1999; Middag et al., 2015b; Moran and Moore, 1991) represent important sources of Al to the deep ocean. Recently, hydrothermal vents (Measures et al., 2015; Resing et al., 2015) were noted as Al sources to the deep Atlantic and Pacific Oceans, with plumes extending at depth over 3000 km in the Pacific Ocean.

25 Removal of Al in oceanic waters occurs through particle scavenging with subsequent sinking of the particulate matter (Orians and Bruland, 1986). The removal is reported to be caused by active scavenging onto opaline frustules of diatoms, as shown in laboratory experiments and supported by positive correlations between orthosilicic acid $(Si(OH)_4)$ and Al in depth profiles upon the sinking and

remineralization of diatomous material (Gehlen et al., 2002; Hydes et al., 1988; Hydes, 1989; Middag et al., 2009; Middag et al., 2015b; Moran and Moore, 1988a). However, *post-mortem* incorporation of Al into the diatoms frustules has also been postulated as an Al removal process (Koning et al., 2007; Vrieling et al., 1999).

5 In the North Atlantic (40° N-65° N) high resolution dAl profiles are scarce prior to the GEOTRACES era (Mawji et al., 2015). In the western North Atlantic reported dAl concentrations range from 1 nM in surface waters up to 27 nM near the seafloor (Hall and Measures, 1998; Middag et al., 2015b). In the eastern North Atlantic dAl concentrations in surface waters range between 1-5 nM (Measures et al., 2008) and in contrast to the western North Atlantic, a dAl mid depth maximum (>30 nM) is observed associated with Mediterranean

10 Overflow Waters (MOW) (Measures et al., 2015; Rolison et al., 2015). Globally, the highest dAl concentrations have been measured in the Mediterranean Sea (up to 174 nM) (Chou and Wollast, 1997; Hydes et al., 1988; Rolison et al., 2015) and the subtropical North Atlantic (up to 60 nM) (Schlosser et al., 2014), while the lowest concentrations (< 1nM) were found in the Southern Ocean (Middag et al., 2011), Pacific Ocean (Orians and Bruland, 1986) and high latitude North Atlantic (Middag et al., 2015b).

15 This manuscript provides an overview of the surface and water column distribution of dAl in the North Atlantic Ocean and Labrador Sea along GEOTRACES section GA01. The sources and sinks of Al for the surface and deep ocean are discussed, and the controls that regulate dAl are discussed in light of $(Si(OH)_4)$ and particulate Al (pAl) distributions.

20 **2. Methods**

2.1. Sampling and processing

The GEOVIDE cruise was conducted as part of the GEOTRACES programme (GA01 section), and sailed on May 15 (2014) from Lisbon (Portugal), passed by the most southern tip of Greenland (June 16, 17) and arrived in St. John´s (Canada) on June 30 (Fig. 1a). A total of 32 stations were sampled for dissolved and

25 particulate trace metals. Seawater was collected using a trace metal clean rosette (TMR, General Oceanics Inc. Model 1018 Intelligent Rosette), attached to a Kevlar line and fitted with 24×12 L GO-FLO bottles (General Oceanics). After recovery, GO-FLO bottles were transferred to a clean container for sampling.

Dissolved Al samples were filtered using 0.2 μm capsule filters (Sartobran 300, Sartorius) or 0.45 μm polyethersulfone filters (Supor®, Pall Gelman), under a slight overpressure (0.2 bar; filtered (Acrovent) N_2

(Air Liquide). Seawater samples were collected in 125 mL low density polyethylene bottles (LDPE; Nalgene), cleaned using a three-step protocol (as per Cutter et al., 2017). After collection, the samples were acidified to pH 1.8 with HCl (ultra-pure acid (UpA), Romil) and double bagged. Samples were shipped to GEOMAR (Kiel, Germany) and analysed in a class 100 clean laboratory. Samples for particulate trace metals

5 (Gourain et al., this issue) were collected on 0.45 μm pore size polyethersulfone (PES) filters (Supor®, Pall Gelman) and stored frozen until analysis in LEMAR (Brest, France). Additionally, total dissolvable Al (TdAl) samples (unfiltered) were collected (May 2014) by hand in 125 mL acid cleaned LDPE bottles (Nalgene) from icebergs (n=11) and surface waters in Godthåbsfjord (n=6) (SW Greenland), acidified to pH ˜1.8 by addition of HCl (UpA, Romil) and stored for 6 months prior to analysis at GEOMAR. After

10 collection, ice samples were defrosted at room temperature in LDPE bags, with the first meltwater discarded to minimize contamination from sample collection, as described by Hopwood et al. (2016).

2.2 Dissolved Al analysis

Samples were analysed using flow injection analysis (FIA) with fluorescence detection as developed by

15 Resing and Measures (1994), and modified by Brown and Bruland (2008). In short, acidified samples were buffered online to pH 5.1 ± 0.1 with a 2 M ammonium acetate buffer (UpA, Romil), and passed over a chelating iminodiacetic acid resin (IDA, Toyopearl AF-Chelate 650M). The loading time was adjusted to 120 s and was extended up to 180 s for samples with low dAl concentrations (<2 nM). After sample loading, the column was rinsed for 70 s with deionised water (18.2 MΩ cm^{-1}, Milli-Q, Millipore) to remove the major

20 seawater anions that interfere with analysis. Subsequently, the preconcentrated dAl was eluted (120 s) from the resin using 0.1 M HCl solution (UpA, Romil) and passed into the reaction stream. Next, the eluent was combined with lumogallion (TCI) in 2 M ammonium acetate buffer. The eluent and lumogallium mixture was passed through a 5 m long reaction coil with external heating to 60°C, supporting the formation of the fluorescent complex. After that, the reagent stream was combined with a 2.5% (volume: volume deionised

25 water) Brij 35% solution (Sigma Aldrich) prior to detection using a fluorometer (Shimadzu RF-10A XL). Emission and excitation wavelengths were set to 484 and 502 nm, respectively. All samples were analysed in duplicate and the concentrations calculated using peak heights.

Calibration was undertaken using standard additions prepared in low trace metal seawater. The different standards were prepared from a stock standard solution of 1 µM prepared from a 1000 ppm Al standard (Merck Millipore). Typically, a calibration was set up with the following standards solutions: 0, 2, 4, 12, 20 and 30 nM. The buffer blank was determined as the difference in counts (arbitrary units) between

5   three samples spiked with increasing amounts of buffer (single, double and triple spike). The system manifold blank was determined as the mean value of two acidified (pH 1.8) samples analysed without buffering. The total blank contribution was calculated by the addition of the buffer and the manifold blank. This blank was subtracted from the results obtained. The detection limit (0.4 nM) was calculated as three times the standard deviation of the manifold blank.

10 The accuracy and precision of the measurements was evaluated by analysis of consensus seawater samples as well as internal reference seawater. GEOTRACES deep (GD) and SaFe S reference seawater were analysed (n=4 and n=9) yielding an average concentration of 17.79 ± 0.26 and 1.85 ± 0.33 nM, respectively, and were in good agreement with the GEOTRACES consensus values as of May 2013 (www.geotraces.org) (SaFe S= 1.67 ± 0.1 nM; GD= 17.7 ± 0.2 nM). A second validation approach of the results was obtained

15 by the comparison of two stations sampled in close proximity in the Iberian Basin by the GEOVIDE cruise (Station 11, 40.33 °N, 12.22 °W) and the GEOTRACES cruise 64PE370 section GA04N (Station 1, 39.73 °N, 14.17 °W). Dissolved Al was analysed using the same analytical technique for both studies. The dAl data from waters deeper than 1000 m were used in order to exclude any seasonal variations and based on the salinity profiles which matched below this depth. The Fisher-based test was used for

20 comparison between profiles as both flow injection data sets were measured with replicates (Middag et al., 2015a). No significant difference (i-p-value= 0.2-0.3) could be determined within analytical uncertainty comparing the two profiles. The dAl dataset has thus been successfully intercalibrated through GEOTRACES, included in the Intermediate Data Product 2017 and submitted to the British Oceanographic Data Center (BODC) (www.bodc.ac.uk).

2.3 Ancillary data

Suspended particles were digested at LEMAR following the protocol of Planquette and Sherrell (2012) and analysed for particulate Al as described in Gourain et al. (this issue). Orthosilicic acid

concentrations were analysed on board using a Bran+Luebbe AA III autoanalyser following Aminot and Kérouel (2007).

A Seabird sensor package 911 mounted to the CTD frame recorded pressure, temperature and salinity data, while a Seabird 43 was used for dissolved oxygen. Salinity and oxygen data were calibrated using

5 analysis of discrete samples with a salinometer (Guildline) and the Winkler method (Carpenter, 1965), respectively.

3. Results and discussion

3.1 Regional and hydrographical settings

10 Along the GEOVIDE section, three biogeochemical provinces (Longhurst, 2010) were investigated: (i) the North Atlantic Subtropical (NAST) region, including the Iberian Basin (IB, Stations 1 to 19); (ii) the North Atlantic Drift (NADR) region, including the Eastern North Atlantic Basin (ENAB, Stations 21 to 26) and Iceland Basin (IcB, Stations 29 to 38); (iii) the Subarctic North Atlantic Artic (SANARCT) including the Irminger Basin (IrB, Stations 40 to 60) and the Labrador Basin (LB, Stations 61 to 71) (Fig. 1a). The salinity

15 distribution and the main water masses in the North Atlantic and Labrador Sea are shown in Fig. 1b. The main water masses used in the discussion of the dAl distribution are the (i) MOW which originates in the Mediterranean Sea, is present at intermediate layers (~500 to 2600 m) on the most eastern part of the section and decreases in salinity and density with increasing distance from Gibraltar (Baringer and Price, 1997); (ii) Iceland Scotland and Denmark Strait Overflow Waters (ISOW and DSOW respectively) which are cold and

20 saline water masses (ISOW = θ of 2.6°C, S of 34.98; DSOW= θ of 1.3°C, S of 34.90) formed in the Norwegian and Nordic seas and produced during the overflow across the sills in the Faroe Bank Channel and over the Iceland-Faroe ridge for the ISOW, and across the Denmark Strait into the IrB for the DSOW (Read, 2000; Swift et al., 1980; Tanhua et al., 2005; Van Aken and De Boer, 1995); (iii) East North Atlantic Central Water (ENACW) which originates in the North Atlantic subtropical gyre by subduction of surface waters

25 (Pollard et al., 1996); (iiii) North East Atlantic Deep Water (NEADW) which is enriched in $Si(OH)_4$ and NO_3^- and present low levels of O_2 and (iiiii) Labrador Sea Water (LSW) which is formed by freshening, cooling and deep convection of the sub-polar Mode Water in the Labrador Sea (Talley and McCartney, 1982). A detailed description of the water masses and mixing figures, obtained through an extended optimum multiple parameter (eOMP) analysis can be found in García-Ibañez et al. (this issue).

3.2 The surface distribution of dAl along the GEOVIDE transect: influence of atmospheric deposition, phytoplankton communities and freshwater sources

5   Figure 2 shows dAl concentrations in surface waters (ca. 15 m depth) along the cruise track, which ranged between 0.54 (Station 26) and 30.99 nM (Station 2). Average surface dAl concentrations decreased from 3.1 ± 1.8 nM (n=5) in the IB to 2.6 ± 2.3 nM (n=4) in the ENAB and 2.3 ± 1.1 nM (n=5) in the IcB, to 1.8 ± 0.9 nM (n=4) and 1.6 ± 1.7 nM (n=3) in the IrB and LB, respectively. Our low surface dAl values agreed with literature values for the ENAB (Barrett et al., 2015; Kramer et al., 2004;

10 Measures et al., 2008; Ussher et al., 2013) and IrB (Middag et al., 2015b), and coincided with low pAl concentrations except over the Greenland shelf (See subsection 3.2.4) (Fig. 2).

3.2.1. Atmospheric deposition

15   In the North Atlantic atmospheric aerosol loading declines with increasing distance from the African dust source regions (e.g. Sahara and Sahel deserts) (Duce et al., 1991; Jickells et al., 2005). The low dAl surface concentrations observed (Fig. 2) in the different basins suggest low aerosol deposition to the study area, which is in line with low aerosol deposition fluxes reported for the GEOVIDE cruise by Shelley et al. (2017). Aerosol deposition is considered as the major source of Al to the surface ocean

20 and modelling studies on global dust deposition indicate a tenfold decrease in atmospheric dust deposition between Portugal and the Labrador Sea (5 to 0.5 g m^{-2} yr^{-1}, values from Mahowald et al., 2005) (Han et al., 2008; Jickells et al., 2005; Mahowald et al., 2005; van Hulten et al., 2014; van Hulten et al., 2013). We performed a one way ANOVA analysis of surface dAl and pAl for the different basins to determine whether atmospheric deposition was the dominant control on surface Al distributions,

25 expecting a decrease in concentrations from east to west. No significance difference was observed (at the p<0.05 level) in surface dAl and pAl between the different basins (dAl: [$F_{(3, 17)} = 0.89$, p= 0.46]; pAl: [$F_{(3, 17)} = 1.79$, p=0.18]), hence additional processes must have controlled the surface distribution of Al along the section.

3.2.2 Dynamic equilibrium between dissolved and particulate Al phases

Biogenic opal production and biogenic particles play an important role in the removal of dAl in the surface ocean as a result of the high particle affinity of dAl. Removal of dAl by biogenic particles therefore represents a mechanism which reduces dAl and increases pAl concentrations in surface waters. During the GEOVIDE cruise, Chl a concentrations increased from the NAST (0.2 to 0.6 mg m^{-3}), via the NARD (0.5 to 1.3 mg m^{-3}) to the ARCT region (up to 5.5 mg m^{-3} at station 61) (Tonnard et al., a, this issue). Along the GEOVIDE transect, diatoms were the dominant phytoplankton taxa in the ENAB, IrB and LB while coccolithophorids were dominant in the IcB (Tonnard et al., a, this issue). Increased pAl to dAl ratios were observed in surface waters where diatoms were dominant (Fig. 6c), as a consequence of dAl incorporation into siliceous shells (Gehlen et al., 2002), preferential scavenging of dAl onto biogenic opal (Moran and Moore, 1988a) and other biogenic particles (Orians and Bruland, 1985). One way ANOVA analysis was performed for the pAl to dAl ratio in the euphotic zone of the four basins which showed high dAl to Si(OH)$_4$ correlations (LB, IrB, IcB and ENAB, see section 3.3.1). The ANOVA test showed significant differences (at the p <0.01 level) between basins [F (3, 38) = 7.9, p=0.0003]. Post hoc comparisons using the Tukey HSD test showed significant differences between the LB and IcB (p <0.01) and ENAB (p <0.05) and between IrB and the IcB (p<0.01). No significant difference was observed between the IrB and the LB and ENAB (p =0.86 and 0.28, respectively), and between ENAB and IcB (p=0.3). Taken together, our results indicate that when diatoms were abundant, as in the IrB and LB (>60% of total phytoplankton community, Tonnard et al., a, this issue), the ratio between pAl and dAl significantly increases due to dAl sorption by biogenic opal. Similar observations have been reported for laboratory studies and in the field where dAl decreased as a function of diatom growth and/or the presence of enhanced quantities of biogenic particles (Hydes, 1979; Kremling, 1985; Kremling and Hydes, 1988; Measures et al., 1986; Measures et al., 1984; Orians and Bruland, 1986; Stoffyn, 1979; van Bennekom, 1981). In addition, the transfer from dAl to pAl has been observed in coastal regions (Brown et al., 2010; Moran and Moore, 1988a) and the North Atlantic (Barrett et al., 2015). Considering the low aerosol deposition and reduced fluvial inputs into the basins (ENAB, IcB,

IrB and LB) we conclude that the observed differences in pAl to dAl ratios were related to diatom abundance.

3.2.3 The Iberian shelf surface waters: Influence of the Tagus estuary

Enhanced surface water dAl concentrations were observed on the Iberian shelf (stations 1, 2 and 4), with average dAl concentrations of 25.5 ± 5.5 nM (n=3) (Fig. 3) which decreased westwards to 5.6 nM (station 11). Previous GEOTRACES cruises close to the Iberian Peninsula (Fig. 3), GA03 (Measures et al., 2015) and 64PE370 (Rolison et al., 2015), observed average surface water dAl concentrations of

10 11.1 ± 2 nM (n=3) and 4.7 ± 2 nM (n=4), respectively (Fig. 3). Higher surface dAl concentrations were observed for the GEOVIDE than for the GA03 and 64PE370 cruises, despite aerosol deposition of Al being one order of magnitude lower during GEOVIDE compared with GA03 (Shelley et al., 2015; Shelley et al., 2017). Salinity profiles for GEOVIDE showed salinity minima (<35) in surface water for stations 1, 2, and 4 (Fig. 4), which suggest a freshwater source. GEOVIDE ship´s ADCP data (Fig. S1)

15 showed that surface waters near the Iberian Peninsula flowed in a northward direction. Therefore, we suggest that the additional source of dAl to surface waters originates from the Tagus estuary, a strongly polluted estuary (Cotté-Krief et al., 2000), located approximately 175 km south from stations 1, 2 and 4. Elevated concentrations of dissolved iron (Tonnard et al., this issue) in the Tagus outflow observed during the GEOVIDE cruise supports an estuarine source of dAl. Wet deposition events registered

20 between stations 1 and 4 during the GEOVIDE cruise (Shelley et al., 2017) formed an additional freshwater source of dAl to surface waters which was superimposed on the Tagus input. Our results indicate that a fraction of riverine dAl can be advected offshore and that dAl is not always effectively removed in estuaries (Hydes, 1979; Maring and Duce, 1987).

25 ### 3.2.4 The Greenland shelf surface waters: Influence of glacial runoff and ice melt

Concentrations of dAl in surface samples collected on the Greenland shelf ranged between 2 to 7 nM, and coincided with reduced salinities (down to 32.2) and enhanced pAl concentrations (up to 62 nM) (Fig. 5a, b and c). Linear regressions between dAl, pAl and salinity for surface samples collected SE

and SW of Greenland displayed correlations above $R^2=0.89$ (Table 1). Aluminium concentrations increased with reduced salinity indicating a freshwater Al source, supplied by ice melt and/or glacial runoff. The ice melt and glacial runoff was delivered by the East Greenland Current (EGC), which flows southwards parallel to the eastern coast of Greenland (Woodgate et al., 1999), carrying sea ice

5 and a smaller fraction of freshwater originating from glacial ice and meltwater (Bacon et al., 2002; Martin and Wadhams, 1999).

Freshwater endmembers (salinity 0) for Al were determined from linear regressions between dAl, pAl and salinity for the eastern (stations 49, 53, 56 and 60; dAl 60.5 ± 9.9 and pAl 773.7 ± 125.6) and western (stations 61, 63 and 64; dAl 6.2 ± 1.2 and pAl 675.1 ± 124.7 nM) Greenland transects (Table

10 1). To determine which source (glacial runoff or ice melt) contributed most strongly to our Al signals in surface waters off the Greenland shelf, we analysed a collection of fjord and iceberg samples from west Greenland. Sea ice Al concentrations were not determined but we anticipate that the sea ice Al endmember would be more similar to Iceberg concentrations than to glacial runoff. Mean total dissolvable Al (unfiltered) iceberg and fjord concentrations were 55 ± 2 nM and 12.8 ± 6 µM,

15 respectively (Table S1). Freshwater Al endmembers (dAl + pAl) were an order of magnitude higher than mean tdAl measured in iceberg samples. Thus, the Al values off Greenland appear to be related to the input from terrestrial runoff enriched with glacial flour. Similar observations were made in Cumberland Bay (Schlosser et al., 2017), and attributed to suspended glacial flour as the main source for enhanced pAl concentrations.

3.3 Overview of spatial distribution of dAl

The section of dAl showed low concentrations in surface waters and an increase with depth (Fig. 6a, b), therefore resembling a nutrient type distribution. The IB formed an exception with maximum dAl (up to

25 38 nM) observed at intermediate depths associated with the MOW (Fig. 6a, b and Fig. S2) (see section 3.4.1). Average dAl depth profiles as well as maximum, minimum, median and quartile (1st and 3rd) dAl values per basin are presented in Fig. 6b. In sub-surface waters between 50 and 500 m depth the median dAl concentrations was lowest in the LB (4.3 nM) and highest in the ENAB (7.6 nM) associated

with East North Atlantic Central Waters (Fig. 6b), with an overall median concentration along the full transect of 5.9 nM (n=132). In the IB observed dAl in sub surface waters compare well with GEOTRACES 64PE370 (Rolison et al., 2015) (Median 7.3 nM for GEOVIDE and 8.2 nM for 64PE370), although they are lower than for GA03 (Measures et al., 2015) (Median 16.4 nM) (Fig 6b).

5 GEOVIDE and 64PE370 cruises sampled in May 2015 and May 2013, respectively, while GA03 sampled in October 2010. Increased aerosol deposition was observed during GA03 (Shelley et al., 2015) in comparison with GEOVIDE (Shelley et al., 2017). Thus, enhanced dAl for GA03 could be related to enhanced removal of dAl in surface waters and concomitant remineralization of biogenic particles following the decline of the late summer-autumn bloom. However, this possible explanation remains

10 speculative. Sub-surface dAl in the IrB compared well between GEOVIDE (Median 4.6 nM) and GA02 (Middag et al., 2015b) (Median 2.0 nM) (Fig. 6b). In deep waters sampled between 500 and 2500 m, the median dAl concentration was lowest in the LB (6.6 nM) and highest in the IB (15.7 nM), with a median concentration along the full GEOVIDE transect of 10.3 nM (n=206). In the IB differences were found in mid waters (Fig. 6b) between GEOVIDE (Median 16.5 nM) and 64PE370 (Median 23.8 nM)

15 and GA03 (Median 32.7 nM) and are linked to a more pronounced presence of MOW for GA03 and 64PE370 than for GEOVIDE (see section 3.4.1). Below 2500 m, the median dAl concentration was lowest in the ENAB (14.4 nM) and highest in the IB (20.9 nM) associated with North East Atlantic Deep Water, with a median concentration along the full transect of 16.7 nM (n=134). Deep concentrations were comparable between GEOVIDE, 64PE370, GA03 and GA02 (Fig. 6b), and

20 displayed similar concentrations on the eastern and western part of the transect as noted before by Middag et al. (2015b) at a latitude of ca. 40°N.

3.3.1 Remineralization versus scavenging in the North Atlantic and Labrador Sea

In the remote oligotrophic regions of the North Atlantic Ocean with enhanced Saharan dust inputs, dAl

25 shows enhanced surface water concentrations with depletion at depth (Measures et al., 2015), typical for a scavenged type element (Bruland et al., 2014). A nutrient type depth distribution of dAl has been reported for the Arctic Ocean (Middag et al., 2009), Mediterranean Sea (Hydes et al., 1988; Rolison et al., 2015b), North Atlantic (Barrett et al., 2012; Measures et al., 2008) and the high latitude North

Atlantic (Middag et al., 2015b) and this vertical distribution coincides with strong correlations between dAl and Si(OH)$_4$ (Hydes et al., 1988; Middag et al., 2015b; Middag et al., 2009; Rolison et al., 2015b). Dissolved Al is removed from surface waters onto particle surfaces (Moore and Millward, 1984; Orians and Bruland, 1985), including diatom cells (Gehlen et al., 2002; Middag et al., 2009) and subsequently

5 released at depth during opal dissolution and the recycling of biogenic particles. In our study region, diatoms dominate the phytoplankton communities at the early stage of the spring bloom (Brown et al., 2003), and are an important producer of biogenic silica (bSiO$_2$) (Nelson et al., 1995) which is the main carrier for scavenged Al (Moran and Moore, 1988b; Stoffyn, 1979). Elevated bSiO$_2$ concentrations and associated high export rates of bSiO$_2$ were measured in the ENAB (up to 1.19 µM BSi) and in the IrB

10 and LB (up to 4.27 and 4.63 µM bSiO$_2$ respectively) (Lemaitre et al., 2017). Dissolved Al and Si(OH)$_4$ displayed strong correlations in all basins (ENAB, IcB, IrB and LB) ($R^2 > 0.76$), except in the IB ($R^2 = 0.2$) which featured Al enrichment from the MOW (See section 3.4.1), the Tagus estuary and the Iberian shelf and margin (see section 3.2.1 and 3.4.2). The large production of biogenic opal and other biogenic particles (e.g. CaCO$_3$ from coccolitophorids) (Lemaitre et al., this issue), the strong correlation between

15 dAl and silicic acid and the increased in dAl concentrations with depth (Fig. 6a and b, see section 3.3) along the cruise track suggests that the net remineralization of dAl from particles was larger than the net removal of dAl from scavenging.

3.4. Dissolved Al enrichment at depth
3.4.1 Mediterranean outflow water (MOW)

The Mediterranean Sea receives large inputs of aerosols which result in elevated dAl concentrations of up to 174 nM, as reported by Hydes et al. (1988). The presence of the MOW was indicated by a mid-depth maximum in salinity (>36) (Fig. 1b), low oxygen concentrations (< 171 µM, data not shown) and a dAl maximum (Fig. 6a and b) at stations 11 to 29, relative to surrounding water masses. The highest

25 dAl concentration (38.7 nM) in the outflow water was observed at station 1 (ca. 900 m deep), in agreement with observations made along GA03 for station USGT10-1 (depth 876 m – dAl = 38.8 nM) (Measures et al., 2015). Figure 7 displays dAl & pAl versus S correlations for the MOW for the neutrally density surface layer (y^n) between 27.6 and 27.8 kg m^{-3}, corresponding to a MOW core depth

between 1000 and 1200 m. In addition, dAl vs S for GA03 and 64PE370 are plotted. The data used in the linear regressions, cover a distance of 1800 km from station 11 to station 29. The coefficients of determination (R^2) observed for dAl & pAl against S are 0.95 and 0.67 (Fig. 7), respectively. The correlations shown in Fig. 7 and the dAl and pAl profiles of station 11 (Fig. S2) indicate that the MOW

5 is highly enriched in dAl and depleted in pAl, and represents a major source of dAl to mid depth waters in the North Atlantic. The good correlation of dAl vs. S and the steady decline of dAl in a westerly direction along the density surface 27.7 kg m^3 suggest that dAl in MOW waters is largely controlled by mixing with surrounding water masses and only to a minor degree by the recycling of particles. Due to this, dAl could be used as a quantitative MOW water mass tracer.

3.4.2 Sediment resuspension

Sediment resuspension due to physical forcing (e.g internal waves and tides, and currents), sediment transport over the shelf, and diffusion of Al-rich pore waters are all deemed to increase Al levels at

15 depth. Enhanced dAl levels have been observed as a result of continental margin inputs for the Drake Passage (Middag et al., 2012) and European shelf (de Jong et al., 2007; Moran and Moore, 1991)**.** Moreover, in the North Atlantic, resuspension of sediments associated with benthic nepheloid layers have been shown to elevate dAl concentrations in comparison to overlying waters (Middag et al., 2015b; Moran and Moore, 1991; Sherrell and Boyle, 1992).

20 On the Iberian and Greenland shelves and margins we observed enhanced dAl concentrations and pAl to dAl ratios (fig. 6a, c). In contrast, on the Newfoundland shelf no enhanced dAl concentrations were observed. On the Iberian shelf and margin enhanced dAl concentrations were observed near the seafloor (station 2: up to 21 nM at z=140 m; station 4: up to 27 nM at z=800 m) associated with enhanced pAl concentrations (up to 1.5 µM at station 2) (Gourain et al., this issue). Likely, the Portugal current

25 (Coelho et al., 2002; Huthnance et al., 2002), and poleward (Frouin et al., 1990) and equatorward upper slope currents (Hall et al., 2000) caused the sediment resuspension responsible for the observed enhanced Al levels. On the Greenland margin and shelf, elevated dAl concentrations were measured at stations 53 and 61 (station 53: up to 17.4 nM at z=180 m,) and coincided with high pAl concentrations

(Up to 73.2 nM). The EGC and WGC are known to produce sediment resuspension. Additionally, Mienert et al. (1993) showed that sediments are transported across the shelf from melt water and runoff. On the Newfoundland shelf and margin, no enhanced dAl levels were observed near the seafloor. However, a large input of pAl was observed (station 78), and pAl concentrations increased from 94.6

5   nM at a depth of 140 m to 550 nM at the seafloor (Gourain et al., this issue). Thus, the enhanced pAl levels could be attributed to sediment resuspension events caused by the south flowing Labrador Current (Mertz et al., 1993) possibly in combination with eddies that could also transfer terrigenous inputs into the Labrador Sea (Chanut et al., 2008; Hátún et al., 2007).

Enhanced dAl concentrations in the bottom layers of several basins (Iceland, Irminger, Labrador)

10   accompanied by an enhanced attenuation signal from the beam transmissometer was indicative of the presence of benthic nepheloid layers which are typically caused by strong bottom currents (Eittreim et al., 1976) (e.g. ISOW and DSOW). Figure 8 shows dAl and transmissometry profiles for stations 26, 42, 69 and 77. Enhanced dAl concentrations near the seafloor coincided with enhanced pAl (Gourain et al., this issue) and a reduced transmissometer signal. In contrast, at station 42 dAl concentrations decreased

15   near the seafloor. Based on the eOMP analysis (Garcia Ibanez et al., this issue), the waters at 2900 m depth (dAl 25.1 nM) had an ISOW contribution of 66% and a residual contribution of DSOW of 2%. In contrast, near the seafloor the contribution of DSOW increased to 91% with a residual ISOW contribution of 6%. Thus, the low dAl concentrations near the seafloor were probably related to low dAl DSOW in comparison with overlaying dAl-rich ISOW as been observed previously by Middag et al.

20   (2015b). Enhanced dAl concentrations with no concomitant decreased in transmissometry percentage (station 77) could indicate that dAl was being released from pore waters.

Overall, the observed enhanced Al concentrations suggest that along the GEOVIDE section the continental shelves and margins acted as a source of Al to adjacent waters. However, dAl concentrations did not always increase when enhanced pAl concentrations were present. These results

25   provide some evidence that occasionally scavenging of dAl onto particles is a dominant process rather than partial dissolution of Al from resuspended sediments. Moreover though, the generally increased Al concentrations in bottom layers suggests that these areas act as a potential source of Al to the North

Atlantic Deep Water as observed in previous works (Measures et al., 2015; Middag et al., 2015b; Moran and Moore, 1991).

3.4.3 Hydrothermal activity

Hydrothermal activity was assessed at station 38 over the Mid Atlantic Ridge. Hydrothermal activity has been reported as a source of dAl to the deep ocean in the Pacific and Atlantic (Measures et al., 2015; Resing et al., 2015). Enhanced concentrations in particulate Al (up to 28 nM), Fe, Ti and Mn and a pFe to pAl ratio similar to the ratio in fresh mid-ocean ridge basalts were observed at station 38

10 (Gourain et al., this issue). No enhanced dAl (Fig. 6a) and dFe (Tonnard et al., b, this issue) concentration was evident. Achterberg et al. (2018) observed enhanced dFe over the Reykjanes ridge and attributed it to hydrothermal sources. Therefore, the minor pAl signature observed at station 38 could be partly related to hydrothermal inputs and resuspension of newly formed oceanic crust.

15 **4. Conclusions**

The dAl cycling in seawater is controlled by the relative strength of its sources and removal processes. At large regional scales, along the GEOVIDE section, the dAl distribution was mostly determined by low aerosol depositions, removal onto biogenic particles and the remineralization of biogenic particles

20 at depth. Yet we show that at smaller regional scales, local sources such as rivers and glacial runoff controlled the dAl signatures. Additionally, sediment resuspension events and the processes of sorption/desorption of dAl onto/from particles were important mechanisms determining the dAl concentrations at sediment-water interface. Our results highlight the importance of phytoplankton (particularly diatoms) abundance and dynamics for determining the dynamics between dissolved and

25 particulate Al phases in surface waters.

Overall, the Al distribution along the GEOVIDE section, in addition to other recent discoveries from the GEOTRACES programme, highlights the complex nature of dAl biogeochemical cycling in seawater as it can resemble either a scavenged or a nutrient type element. As a result of the high resolution sampling programme we demonstrate that dAl distributions are controlled by water mass mixing (as for the

Mediterranean Overflow Water). The large sets of parameters measured on each GEOTRACES cruise will allow us, in the coming years, to examine the global ocean dAl cycling from a holistic perspective.

5   **Acknowledgments**

We are greatly thankful to the captain, Gilles Ferrand, and crew of the N/O Pourquoi Pas? for their help during the *GEOVIDE* mission. Many thanks to T. Browning for valuable comments which helped to improve the manuscript. We would like to give a special thanks to Pierre Branellec, Michel Hamon,
10   Catherine Kermabon, Philippe Le Bot, Stéphane Leizour, Olivier Ménage (Laboratoire de Physique des Oceans et Spatiale), Fabien Pérault and Emmanuel de Saint Léger (Division Technique de l'INSU, Brest, France) for their technical expertise during clean CTD deployments and to Catherine Schmechtig for the GEOVDIE database management. We also acknowledge Emilie Grosteffan, Manon Le Goff, Morgane Galinari, and Paul Tréguer for the analysis of nutrients. Greg Cutter is also strongly
15   acknowledged for his help in setting up the new French clean sampling system. This work was supported by GEOMAR, a PhD Fellowship of the Department of Scientific Politics of the Basque government to JLMB, the French National Research Agency (ANR-13-BS06-0014, ANR-12-PDOC-0025-01), the French National Centre for Scientific Research (CNRS-LEFE-CYBER), the LabexMER (ANR-10-LABX-19), and IFREMER. We acknowledge the Helmholtz Association for financing the
20   publication costs for this manuscript.

References

Aminot, A. and Kérouel, R.: Dosage automatique des nutriments dans les eaux marines: méthodes en flux continu, Editions Quae, 2007.
Bacon, S., Reverdin, G., Rigor, I. G., and Snaith, H. M.: A freshwater jet on the east Greenland shelf, Journal of Geophysical Research:
25   Oceans, 107,doi: 10.1029/2001JC000935, 2002.
Baringer, M. O. N. and Price, J. F.: Mixing and spreading of the Mediterranean outflow, Journal of Physical Oceanography, 27, 1654-1677,doi: 10.1175/1520-0485(1997)027<1654:MASOTM>2.0.CO;2, 1997.
Barrett, P. M., Resing, J. A., Buck, N. J., Landing, W. M., Morton, P. L., and Shelley, R. U.: Changes in the distribution of Al and particulate Fe along A16N in the eastern North Atlantic Ocean between 2003 and 2013: Implications for changes in dust deposition,
30   Marine Chemistry, 177, 57-68,doi: 10.1016/j.marchem.2015.02.009, 2015.
Brown, L., Sanders, R., Savidge, G., and Lucas, C. H.: The uptake of silica during the spring bloom in the Northeast Atlantic Ocean, Limnology and Oceanography, 48, 1831-1845,doi: 10.4319/lo.2003.48.5.1831, 2003.

Brown, M. T. and Bruland, K. W.: An improved flow-injection analysis method for the determination of dissolved aluminum in seawater, Limnol. Oceanogr. Methods, 6, 87-95,doi: 10.4319/lom.2008.6.87, 2008.

Brown, M. T., Lippiatt, S. M., and Bruland, K. W.: Dissolved aluminum, particulate aluminum, and silicic acid in northern Gulf of Alaska coastal waters: Glacial/riverine inputs and extreme reactivity, Marine Chemistry, 122, 160-175,doi: 10.1016/j.marchem.2010.04.002, 2010.

Bruland, K., Middag, R., and Lohan, M.: Controls of trace metals in seawater. In 'Treatise on Geochemistry'.(Eds H. Holland and K. Turekian.) pp. 19–51. Elsevier: Amsterdam, Netherlands, 2014.

Carpenter, J. H.: The accuracy of the Winkler method for dissolved oxygen analysis, Limnology and Oceanography, 10, 135-140,doi: 10.4319/lo.1965.10.1.0135, 1965.

Chanut, J., Barnier, B., Large, W., Debreu, L., Penduff, T., Molines, J. M., and Mathiot, P.: Mesoscale eddies in the Labrador Sea and their contribution to convection and restratification, Journal of Physical Oceanography, 38, 1617-1643,doi: 10.1175/2008JPO3485.1, 2008.

Chou, L. and Wollast, R.: Biogeochemical behavior and mass balance of dissolved aluminum in the western Mediterranean Sea, Deep Sea Research Part II: Topical Studies in Oceanography, 44, 741-768,doi: 10.1016/S0967-0645(96)00092-6, 1997.

Coelho, H., Neves, R., White, M., Leitao, P., and Santos, A.: A model for ocean circulation on the Iberian coast, Journal of Marine Systems, 32, 153-179,doi: 10.1016/S0924-7963(02)00032-5, 2002.

Cotté-Krief, M.-H., Guieu, C., Thomas, A.J., and Martin, J.-M.: Sources of Cd, Cu, Ni, Zn in Portuguese coastal waters, Marine Chemistry , 107, 120-142, doi: 10.11016/S0304-4203(00)00049-9, 2000.

Cutter, G., Casciotti, K., Croot, P., Geibert, W., Heimburger, L. E., Lohan, M., Planquette, H., and van de Floerdt, T.: sampling and the Sample-handling Protocols for GEOTRACES Cruises, 2017.

de Jong, J. T., Boyé, M., Gelado-Caballero, M. D., Timmermans, K. R., Veldhuis, M. J., Nolting, R. F., Van den Berg, C. M., and de Baar, H. J.: Inputs of iron, manganese and aluminium to surface waters of the Northeast Atlantic Ocean and the European continental shelf, Marine Chemistry, 107, 120-142,doi: 10.1016/j.marchem.2007.05.007, 2007.

Duce, R., Liss, P., Merrill, J., Atlas, E., Buat-Menard, P., Hicks, B., Miller, J., Prospero, J., Arimoto, R., and Church, T.: The atmospheric input of trace species to the world ocean, Global biogeochemical cycles, 5, 193-259,doi: 10.1029/91GB01778, 1991.

Eittreim, S., Thorndike, E. M., and Sullivan, L.: Turbidity distribution in the Atlantic Ocean, Deep Sea Research and Oceanographic Abstracts, 23, 1115-1127,doi: 10.1016/0011-7471(76)90888-3, 1976.

Frouin, R., Fiúza, A. F. G., Ambar, I., and Boyd, T. J.: Observations of a poleward surface current off the coasts of Portugal and Spain during winter, Journal of Geophysical Research: Oceans, 95, 679-691,doi: 10.1029/JC095iC01p00679, 1990.

Gehlen, M., Beck, L., Calas, G., Flank, A.-M., Van Bennekom, A., and Van Beusekom, J.: Unraveling the atomic structure of biogenic silica: evidence of the structural association of Al and Si in diatom frustules, Geochimica et Cosmochimica Acta, 66, 1601-1609,doi: 10.1016/S0016-7037(01)00877-8, 2002.

Guerzoni, S., Molinaroli, E., and Chester, R.: Saharan dust inputs to the western Mediterranean Sea: depositional patterns, geochemistry and sedimentological implications, Deep Sea Research Part II: Topical Studies in Oceanography, 44, 631-654,doi: 10.1016/S0967-0645(96)00096-3, 1997.

Hall, I., Schmidt, S., McCave, I., and Reyss, J.: Particulate matter distribution and disequilibrium along the Northern Iberian Margin: implications for particulate organic carbon export, Deep Sea Research Part I: Oceanographic Research Papers, 47, 557-582,doi: 10.1016/S0967-0637(99)00065-5, 2000.

Hall, I. R. and Measures, C.: The distribution of Al in the IOC stations of the North Atlantic and Norwegian Sea between 52° and 65° North, Marine chemistry, 61, 69-85,doi: 10.1016/S0304-4203(98)00008-5, 1998.

Han, Q., Moore, J. K., Zender, C., Measures, C., and Hydes, D.: Constraining oceanic dust deposition using surface ocean dissolved Al, Global biogeochemical cycles, 22,doi: 10.1029/2007GB002975, 2008.

Hátún, H., Eriksen, C. C., and Rhines, P. B.: Buoyant eddies entering the Labrador Sea observed with gliders and altimetry, Journal of Physical Oceanography, 37, 2838-2854,doi: 10.1175/2007JPO3567.1, 2007.

Hesse, R., Klauck, I., Khodabakhsh, S., and Piper, D.: Continental slope sedimentation adjacent to an ice margin. III. The upper Labrador Slope, Marine Geology, 155, 249-276,doi: 10.1016/S0025-3227(98)00054-1, 1999.

Hopwood, M. J., Connelly, D. P., Arendt, K. E., Juul-Pedersen, T., Stinchcombe, M. C., Meire, L., Esposito, M., and Krishna, R.: Seasonal changes in Fe along a glaciated Greenlandic fjord, Frontiers in Earth Science, 4, 15,doi: 10.3389/feart.2016.00015, 2016.

Huthnance, J. M., Van Aken, H. M., White, M., Barton, E. D., Le Cann, B., Coelho, E. F., Fanjul, E. A., Miller, P., and Vitorino, J.: Ocean margin exchange—water flux estimates, Journal of Marine Systems, 32, 107-137,doi: 10.1016/S0924-7963(02)00034-9, 2002.

Hydes, D., De Lange, G., and De Baar, H.: Dissolved aluminium in the Mediterranean, Geochimica et Cosmochimica Acta, 52, 2107-2114,doi: 10.1016/0016-7037(88)90190-1, 1988.

Hydes, D. J.: Aluminum in seawater: Control by inorganic processes, Science, 205, 1260-1262,doi: 10.1126/science.205.4412.1260 1979.

Hydes, D. J.: Seasonal variation in dissolved aluminium concentrations in coastal waters and biological limitation of the export of the riverine input of aluminium to the deep sea, Continental Shelf Research, 9, 919-929,doi: 10.1016/0278-4343(89)90065-4, 1989.

Jeandel, C., Peucker-Ehrenbrink, B., Jones, M. T., Pearce, C. R., Oelkers, E. H., Godderis, Y., Lacan, F., Aumont, O., and Arsouze, T.: Ocean margins: The missing term in oceanic element budgets?, Eos, Transactions American Geophysical Union, 92, 217-218,doi: 10.1029/2011EO260001, 2011.

Jickells, T. D., An, Z. S., Andersen, K. K., Baker, A. R., Bergametti, G., Brooks, N., Cao, J. J., Boyd, P. W., Duce, R. A., Hunter, K. A., Kawahata, H., Kubilay, N., laRoche, J., Liss, P. S., Mahowald, N., Prospero, J. M., Ridgwell, A. J., Tegen, I., and Torres, R.: Global iron connections between desert dust, ocean biogeochemistry, and climate, Science, 308, 67-71,doi: 10.1126/science.1105959, 2005.

Koning, E., Gehlen, M., Flank, A.-M., Calas, G., and Epping, E.: Rapid post-mortem incorporation of aluminum in diatom frustules: Evidence from chemical and structural analyses, Marine Chemistry, 106, 208-222,doi: 10.1016/j.marchem.2006.06.009, 2007.

Kramer, J., Laan, P., Sarthou, G., Timmermans, K. R., and de Baar, H. J. W.: Distribution of dissolved aluminium in the high atmospheric input region of the subtropical waters of the North Atlantic Ocean, Marine Chemistry, 88, 85-101,doi: 10.1016/j.marchem.2004.03.009, 2004.

Kremling, K.: The distribution of cadmium, copper, nickel, manganese, and aluminium in surface waters of the open Atlantic and European shelf area, Deep Sea Research Part A. Oceanographic Research Papers, 32, 531-555,doi: 10.1016/0198-0149(85)90043-3, 1985.

Kremling, K. and Hydes, D.: Summer distribution of dissolved Al, Cd, Co, Cu, Mn and Ni in surface waters around the British Isles, Continental Shelf Research, 8, 89-105,doi: 10.1016/0278-4343(88)90026-X, 1988.

Lemaitre, N., Planquette, H., Planchon, F., Sarthou, G., Jacquet, S., García-Ibáñez, M., Gourain, A., Cheize, M., Monin, L., André, L., Laha, P., Terryn, H., and Dehairs, F.: Particulate barium tracing significant mesopelagic carbon remineralisation in the North Atlantic, 2017.

Longhurst, A. R.: Ecological geography of the Sea, The Atlantic Ocean, Academic Press, chapter 9,doi: 10.1016/B978-012455521-1/50010-3, 2010.

Mahowald, N. M., Baker, A. R., Bergametti, G., Brooks, N., Duce, R. A., Jickells, T. D., Kubilay, N., Prospero, J. M., and Tegen, I.: Atmospheric global dust cycle and iron inputs to the ocean, Global Biogeochemical Cycles, 19,doi: 10.1029/2004GB002402, 2005.

Maring, H. B. and Duce, R. A.: The impact of atmospheric aerosols on trace metal chemistry in open ocean surface seawater, 1. Aluminum, Earth and Planetary Science Letters, 84, 381-392,doi: 10.1016/0012-821X(87)90003-3, 1987.

Martin, T. and Wadhams, P.: Sea-ice flux in the East Greenland Current, Deep Sea Research Part II: Topical Studies in Oceanography, 46, 1063-1082,doi: 10.1016/S0967-0645(99)00016-8, 1999.

Mawji, E. and Schlitzer, R. and Dodas, E. M. and Abadie, C. and Abouchami, W. and Anderson, R. F. and Baars, O. and Bakker, K. and Baskaran, M. and Bates, N. R. and Bluhm, K. and Bowie, A. and Bown, J. and Boye, M. and Boyle, E. A. and Branellec, P. and Bruland, K. W. and Brzezinski, M. A. and Bucciarelli, E. and Buesseler, K. and Butler, E. and Cai, P. and Cardinal, D. and Casciotti, K. and Chaves, J. and Cheng, H. and Chever, F. and Church, T. M. and Colman, A. S. and Conway, T. M. and Croot, P. L. and Cutter, G. A. and de Baar, H. J. W. and de Souza, G. F. and Dehairs, F. and Deng, F. and Dieu, H. T. and Dulaquais, G. and Echegoyen-Sanz, Y. and Lawrence Edwards, R. and Fahrbach, E. and Fitzsimmons, J. and Fleisher, M. and Frank, M. and Friedrich, J. and Fripiat, F. and Galer, S. J. G. and Gamo, T. and Solsona, E. G. and Gerringa, L. J. A. and Godoy, J. M. and Gonzalez, S. and Grosssteffan, E. and Hatta, M. and Hayes, C. T. and Heller, M. I. and Henderson, G. and Huang, K.-F. and Jeandel, C. and Jenkins, W. J. and John, S. and Kenna, T. C. and Klunder, M. and Kretschmer, S. and Kumamoto, Y. and Laan, P. and Labatut, M. and Lacan, F. and Lam, P. J. and Lannuzel, D. and le Moigne, F. and Lechtenfeld, O. J. and Lohan, M. C. and Lu, Y. and Masqué, P. and McClain, C. R. and Measures, C. and Middag, R. and Moffett, J. and Navidad, A. and Nishioka, J. and Noble, A. and Obata, H. and Ohnemus, D. C. and Owens, S. and Planchon, F. and Pradoux, C. and Puigcorbé, V. and Quay, P. and Radic, A. and Rehkämper, M. and Remenyi, T. and Rijkenberg, M. J. A. and Rintoul, S. and Robinson, L. F. and Roeske, T. and Rosenberg, M. and van der Loeff, M. R. and Ryabenko, E. and Saito, M. A. and Roshan, S. and Salt, L. and Sarthou, G. and Schauer, U. and Scott, P. and Sedwick, P. N. and Sha, L. and Shiller, A. M. and Sigman, D. M. and Smethie, W. and Smith, G. J. and Sohrin, Y. and Speich, S. and Stichel, T. and Stutsman, J. and Swift, J. H. and Tagliabue, A. and Thomas, A. and Tsunogai, U. and Twining, B. S. and van Aken, H. M. and van Heuven, S. and van Ooijen, J. and van Weerlee, E. and Venchiarutti, C. and Voelker, A. H. L. and Wake, B. and Warner, M. J. and Woodward, E. M. S. and Wu, J. and Wyatt, N. and Yoshikawa, H. and Zheng, X.-Y. and Xue, Z. and Zieringer, M. and Zimmer, L. A.: The GEOTRACES Intermediate Data Product 2014, Marine Chemistry, 177, Part 1, 1-8,doi: 10.1016/j.marchem.2015.04.005, 2015.

Measures, C., Brown, M., and Vink, S.: Dust deposition to the surface waters of the western and central North Pacific inferred from surface water dissolved aluminum concentrations, Geochemistry, Geophysics, Geosystems, 6,doi: 10.1029/2005GC000922, 2005.

Measures, C. and Edmond, J.: Aluminium in the South Atlantic: steady state distribution of a short residence time element, Journal of Geophysical Research: Oceans (1978–2012), 95, 5331-5340,doi: 10.1029/JC095iC04p05331, 1990.

Measures, C., Edmond, J., and Jickells, T.: Aluminium in the northwest Atlantic, Geochimica et Cosmochimica Acta, 50, 1423-1429,doi: 10.1016/0016-7037(86)90315-7, 1986.

Measures, C., Grant, B., Khadem, M., Lee, D., and Edmond, J.: Distribution of Be, Al, Se and Bi in the surface waters of the western North Atlantic and Caribbean, Earth and planetary science letters, 71, 1-12,doi: 10.1016/0012-821X(84)90047-5, 1984.

Measures, C., Hatta, M., Fitzsimmons, J., and Morton, P.: Dissolved Al in the zonal N Atlantic section of the US GEOTRACES 2010/2011 cruises and the importance of hydrothermal inputs, Deep Sea Research Part II: Topical Studies in Oceanography, 116, 176-186,doi: 10.1016/j.dsr2.2014.07.006, 2015.

Measures, C., Landing, W., Brown, M., and Buck, C.: High-resolution Al and Fe data from the Atlantic Ocean CLIVAR-CO2 Repeat Hydrography A16N transect: Extensive linkages between atmospheric dust and upper ocean geochemistry, Global Biogeochemical Cycles, 22,doi: 10.1029/2007GB003042, 2008.

Measures, C. and Vink, S.: On the use of dissolved aluminum in surface waters to estimate dust deposition to the ocean, Global biogeochemical cycles, 14, 317-327,doi: 10.1029/1999GB001188, 2000.

Measures, C. I. and Brown, E. T.: Estimating Dust Input to the Atlantic Ocean Using Surface Water Aluminium Concentrations. In: The Impact of Desert Dust Across the Mediterranean, Guerzoni, S. and Chester, R. (Eds.), Springer Netherlands, Dordrecht, 1996.

Mertz, G., Narayanan, S., and Helbig, J.: The freshwater transport of the Labrador Current, Atmosphere-Ocean, 31, 281-295,doi: 10.1080/07055900.1993.9649472, 1993.

Middag, R., Baar, H. d., Laan, P., and Huhn, O.: The effects of continental margins and water mass circulation on the distribution of dissolved aluminum and manganese in Drake Passage, Journal of Geophysical Research: Oceans (1978–2012), 117,doi: 10.1029/2011JC007434, 2012.

Middag, R., de Baar, H. J. W., Laan, P., and Bakker, K.: Dissolved aluminium and the silicon cycle in the Arctic Ocean, Marine Chemistry, 115, 176-195,doi: 10.1016/j.marchem.2009.08.002, 2009.

Middag, R., Séférian, R., Conway, T., John, S., Bruland, K., and de Baar, H.: Intercomparison of dissolved trace elements at the Bermuda Atlantic Time Series station, Marine Chemistry, doi: 10.1016/j.marchem.2015.06.014, 2015a.doi: 10.1016/j.marchem.2015.06.014, 2015a.

Middag, R., Van Hulten, M., Van Aken, H., Rijkenberg, M., Gerringa, L., Laan, P., and De Baar, H.: Dissolved aluminium in the ocean conveyor of the West Atlantic Ocean: effects of the biological cycle, scavenging, sediment resuspension and hydrography, Marine Chemistry, 177, 69-86,doi: 10.1029/2011JC007434, 2015b.

Middag, R., van Slooten, C., de Baar, H. J. W., and Laan, P.: Dissolved aluminium in the Southern Ocean, Deep Sea Research Part II: Topical Studies in Oceanography, 58, 2647-2660,doi: 10.1016/j.dsr2.2011.03.001, 2011.

Mienert, J., Thiede, J., Kenyon, N., and Hollender, F. J.: Polar continental margins: studies off East Greenland, EOS, Transactions American Geophysical Union, 74, 225-236, 1993.

Moran, S. and Moore, R.: Temporal variations in dissolved and particulate aluminum during a spring bloom, Estuarine, Coastal and Shelf Science, 27, 205-215,doi: 10.1016/0272-7714(88)90090-X, 1988a.

Moran, S. B. and Moore, R. M.: Evidence from mesocosm studies for biological removal of dissolved aluminium from sea water, Nature, 335, 706-708,doi: 10.1038/335706a0, 1988b.

Moran, S. B. and Moore, R. M.: The potential source of dissolved aluminum from resuspended sediments to the North Atlantic Deep Water, Geochimica et Cosmochimica Acta, 55, 2745-2751,doi: 10.1016/0016-7037(91)90441-7, 1991.

Orians, K. J. and Bruland, K. W.: The biogeochemistry of aluminum in the Pacific Ocean, Earth and planetary science letters, 78, 397-410,doi: 10.1016/0012-821X(86)90006-3, 1986.

Orians, K. J. and Bruland, K. W.: Dissolved aluminium in the central North Pacific, Nature, 316, 427-429,doi: 10.1038/316427a0, 1985.

Planquette, H. and Sherrell, R. M.: Sampling for particulate trace element determination using water sampling bottles: methodology and comparison to in situ pumps, Limnology and Oceanography: methods, 10, 367-388,doi: 10.4319/lom.2012.10.367, 2012.

Pollard, R. T., Griffiths, M.J., Cunningham, S.A., Read, J.F., Perez, F.F. and Rios, A.F.: Vivaldi 1991- A study of the formation, circulation and ventilation of Eastern North Atlantic Central Water, Progress in oceanography 37, 167-172, doi: 10.1016/S0079-6611(96)00008-0, 1996.

Prospero, J. M. and Carlson, T. N.: Vertical and areal distribution of Saharan dust over the western equatorial North Atlantic Ocean, Journal of Geophysical Research, 77, 5255-5265,doi: 10.1029/JC077i027p05255, 1972.

Read, J.: CONVEX-91: water masses and circulation of the Northeast Atlantic subpolar gyre, Progress in Oceanography, 48, 461-510,doi: 10.1016/S0079-6611(01)00011-8, 2000.

Resing, J. A. and Measures, C. I.: Fluorometric Determination of Al in Seawater by Flow Injection Analysis with In-Line Preconcentration, Analytical Chemistry, 66, 4105-4111,doi: 10.1021/ac00094a039, 1994.

Resing, J. A., Sedwick, P. N., German, C. R., Jenkins, W. J., Moffett, J. W., Sohst, B. M., and Tagliabue, A.: Basin-scale transport of hydrothermal dissolved metals across the South Pacific Ocean, Nature, 523, 200-203,doi: 10.1038/nature14577, 2015.

Rijkenberg, M. J. A., de Baar, H. J. W., Bakker, K., Gerringa, L. J. A., Keijzer, E., Laan, M., Laan, P., Middag, R., Ober, S., van Ooijen, J., Ossebaar, S., van Weerlee, E. M., and Smit, M. G.: "PRISTINE", a new high volume sampler for ultraclean sampling of trace metals and isotopes, Marine Chemistry, 177, Part 3, 501-509,doi: 10.1016/j.marchem.2015.07.001, 2015.

Roberson, C. E. and Hem, J. D.: Solubility of aluminum in the presence of hydroxide, fluoride, and sulfate, USGPO, 1969.

Rolison, J., Middag, R., Stirling, C., Rijkenberg, M., and De Baar, H.: Zonal distribution of dissolved aluminium in the Mediterranean Sea, Marine Chemistry, 177, 87-100,doi: 10.1016/j.marchem.2015.05.001, 2015.

Rudnick, R. and Gao, S.: Composition of the continental crust, Treatise on geochemistry, 3, 659,doi: 10.1016/B0-08-043751-6/03016-4, 2003.

Schlitzer, R., Ocean Data View, online: https://odv.awi.de, [24 Nov 2017], 2017.

Schlosser, C., Klar, J. K., Wake, B. D., Snow, J. T., Honey, D. J., Woodward, E. M. S., Lohan, M. C., Achterberg, E. P., and Moore, C. M.: Seasonal ITCZ migration dynamically controls the location of the (sub)tropical Atlantic biogeochemical divide, Proceedings of the National Academy of Sciences, 111, 1438-1442,doi: 10.1073/pnas.1318670111, 2014.

Schlosser, C., Schmidt, K., Aquilina, A., Homoky, W. B., Castrillejo, M., Mills, R. A., Patey, M. D., Fielding, S., Atkinson, A., and Achterberg, E. P.: Mechanisms of dissolved and labile particulate iron supply to shelf waters and phytoplankton blooms off South Georgia, Southern Ocean, Biogeosciences Discussions, doi: 10.5194/bg-2017-299. , 2017. 1-49,doi: 10.5194/bg-2017-299. , 2017.

Shelley, R. U., Morton, P. L., and Landing, W. M.: Elemental ratios and enrichment factors in aerosols from the US-GEOTRACES North Atlantic transects, Deep Sea Research Part II: Topical Studies in Oceanography, 116, 262-272,doi: 10.1016/j.dsr2.2014.12.005, 2015.

Shelley, R. U., Roca-Martí, M., Castrillejo, M., Masqué, P., Landing, W. M., Planquette, H., and Sarthou, G.: Quantification of trace element atmospheric deposition fluxes to the Atlantic Ocean (> 40° N; GEOVIDE, GEOTRACES GA01) during spring 2014, Deep Sea Research Part I: Oceanographic Research Papers, 119, 34-49,doi: 10.1016/j.dsr.2016.11.010, 2017.

Sherrell, R. M. and Boyle, E. A.: The trace metal composition of suspended particles in the oceanic water column near Bermuda, Earth and Planetary Science Letters, 111, 155-174,doi: 10.1016/0012-821X(92)90176-V, 1992.

Stoffyn, M.: Biological control of dissolved aluminum in seawater: experimental evidence, Science, 203, 651-653,doi: 10.1126/science.203.4381.651 1979.

Stoffyn, M. and Mackenzie, F. T.: Fate of dissolved aluminum in the oceans, Marine chemistry, 11, 105-127,doi: 10.1016/0304-4203(82)90036-6, 1982.

Swift, J. H., Aagaard, K., and Malmberg, S.-A.: The contribution of the Denmark Strait overflow to the deep North Atlantic, Deep Sea Research Part A. Oceanographic Research Papers, 27, 29-42,doi: 10.1016/0198-0149(80)90070-9, 1980.

Talley, L. D. and McCartney, M. S.: Distribution and Circulation of Labrador Sea Water, Journal of Physical Oceanography, 12, 1189-1205,doi: 10.1175/1520-0485(1982)012<1189:DACOLS>2.0.CO;2, 1982.

Tanhua, T., Olsson, K. A., and Jeansson, E.: Formation of Denmark Strait overflow water and its hydro-chemical composition, Journal of Marine Systems, 57, 264-288,doi: 10.1016/j.jmarsys.2005.05.003, 2005.

Ussher, S. J., Achterberg, E. P., Powell, C., Baker, A. R., Jickells, T. D., Torres, R., and Worsfold, P. J.: Impact of atmospheric deposition on the contrasting iron biogeochemistry of the North and South Atlantic Ocean, Global Biogeochemical Cycles, doi: 10.1002/gbc.20056, 2013. n/a-n/a,doi: 10.1002/gbc.20056, 2013.

Van Aken, H. and De Boer, C.: On the synoptic hydrography of intermediate and deep water masses in the Iceland Basin, Deep Sea Research Part I: Oceanographic Research Papers, 42, 165-189,doi: 10.1016/0967-0637(94)00042-Q, 1995.

van Bennekom, A. J.: On the role of aluminium in the dissolution kinetics of diatom frustules, 1981, 445-455.

van Hulten, M. M. P., Sterl, A., Middag, R., de Baar, H. J. W., Gehlen, M., Dutay, J. C., and Tagliabue, A.: On the effects of circulation, sediment resuspension and biological incorporation by diatoms in an ocean model of aluminium*, Biogeosciences, 11, 3757-3779,doi: 10.5194/bg-11-3757-2014, 2014.

van Hulten, M. M. P., Sterl, A., Tagliabue, A., Dutay, J. C., Gehlen, M., de Baar, H. J. W., and Middag, R.: Aluminium in an ocean general circulation model compared with the West Atlantic Geotraces cruises, Journal of Marine Systems, 126, 3-23,doi: 10.1016/j.jmarsys.2012.05.005, 2013.

Vink, S. and Measures, C. I.: The role of dust deposition in determining surface water distributions of Al and Fe in the South West Atlantic, Deep Sea Research Part II: Topical Studies in Oceanography, 48, 2787-2809,doi: 10.1016/S0967-0645(01)00018-2, 2001.

Vrieling, E. G., Poort, L., Beelen, T. P., and Gieskes, W. W.: Growth and silica content of the diatoms Thalassiosira weissflogii and Navicula salinarum at different salinities and enrichments with aluminium, European journal of phycology, 34, 307-316, 1999.

Woodgate, R. A., Fahrbach, E., and Rohardt, G.: Structure and transports of the East Greenland Current at 75 N from moored current meters, Journal of Geophysical Research: Oceans, 104, 18059-18072,doi: 10.1029/1999JC900146, 1999.

a)

b)
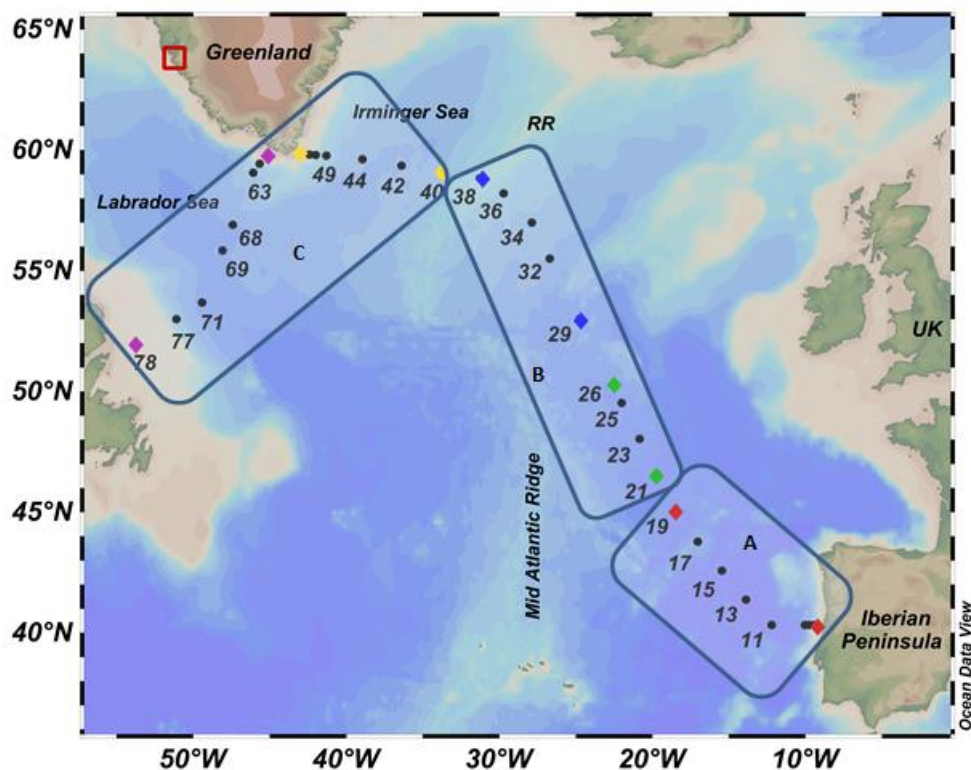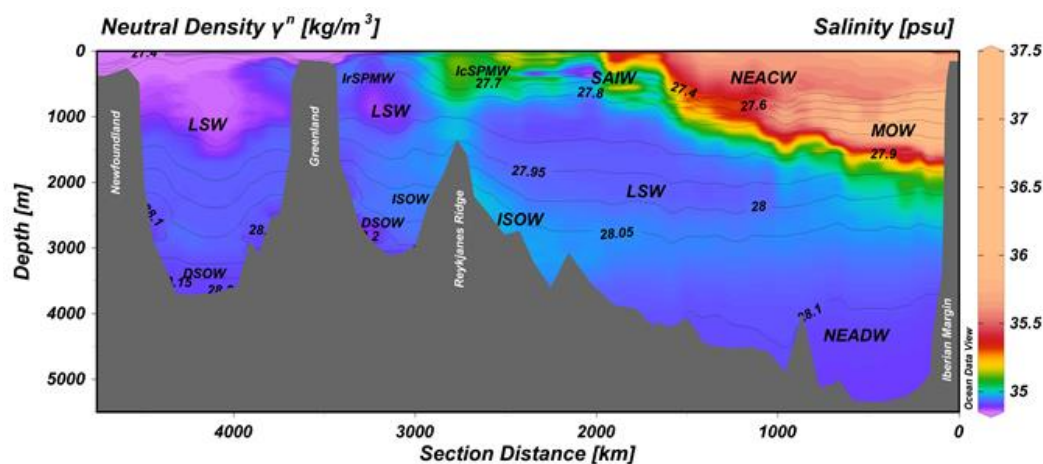
Figure 1: a) The cruise track along the North Atlantic and the Labrador Sea. Numbers represent station numbers. For reference to station numbers on the Iberian and Greenland shelf please refer to figures 3 and 5. Black boxes represent the different biogeochemical provinces: A: North Atlantic Subtropical (NAST); B: North Atlantic Drift (NADR); C: Atlantic Artic (ARCT). Diamonds represent boundaries between different basins: Red: Iberian basin; Green: East North Atlantic basin; Blue: Iceland basin; Yellow: Irminger basin; Purple: Labrador basin. Red box in SW Greenland represent the position of the Godthåbsfjord. RR: Reykjanes Ridge. b) Cross-section plot of salinity along GEOVIDE. Annotations represent main water masses in the study

region. Isolines represent layers of equal neutral density (γ^n). DSOW, Denmark Strait Overflow Water; ISOW, Iceland Scotland Overflow Water; LSW, Labrador Sea Water; MOW, Mediterranean Overflow Water; NEACW, North East Atlantic Central Water; NEADW, North East Atlantic Deep Water; IcSPMW, Iceland Sub Polar Mode Water; IrSPMW, Irminger Sub Polar Mode Water; SAIW, Sub Artic Intermediate Water. Plots created in Ocean Data View (Schlitzer, 2017).
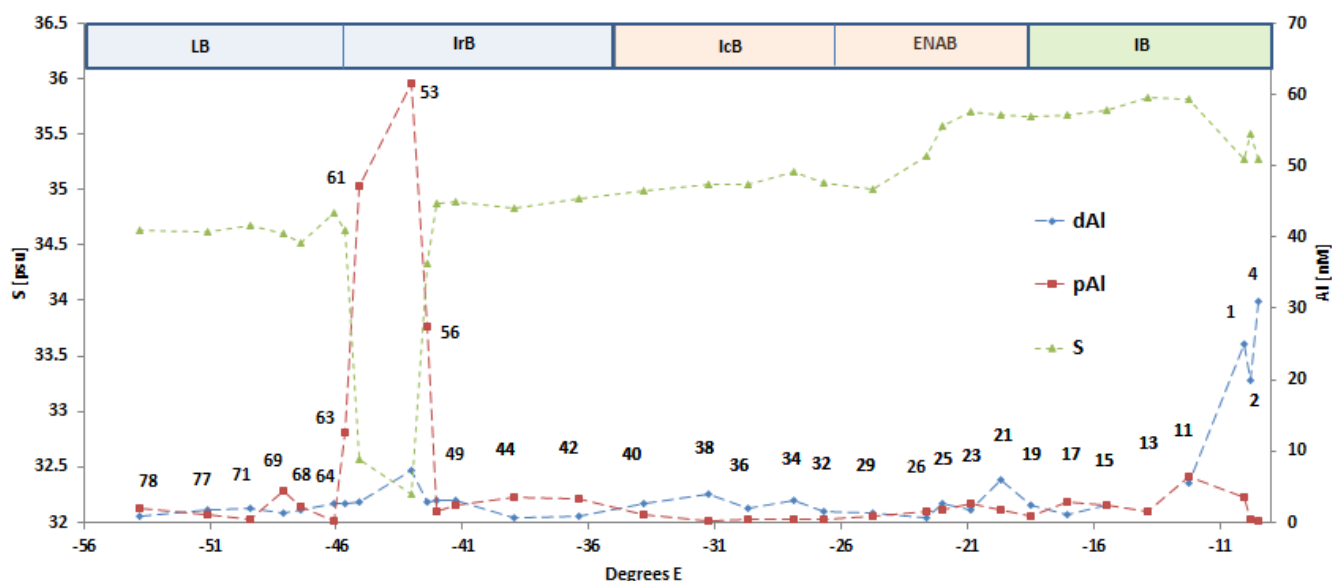
Figure 2: Surface distribution (± 15 meters) of dissolved Al (dAl), particulate Al (pAl) (Gourain et al.,this issue) and salinity along the GEOVIDE section. Boxes represent biogeochemical provinces: Green: NAST; Orange: NADR; Blue: ARCT. Abbreviations in the boxes represent the different basins. IB: Iberian basin; ENAB: East North Atlantic basin; IcB: Iceland basin; IrB: Irminger basin; LB: Labrador basin.
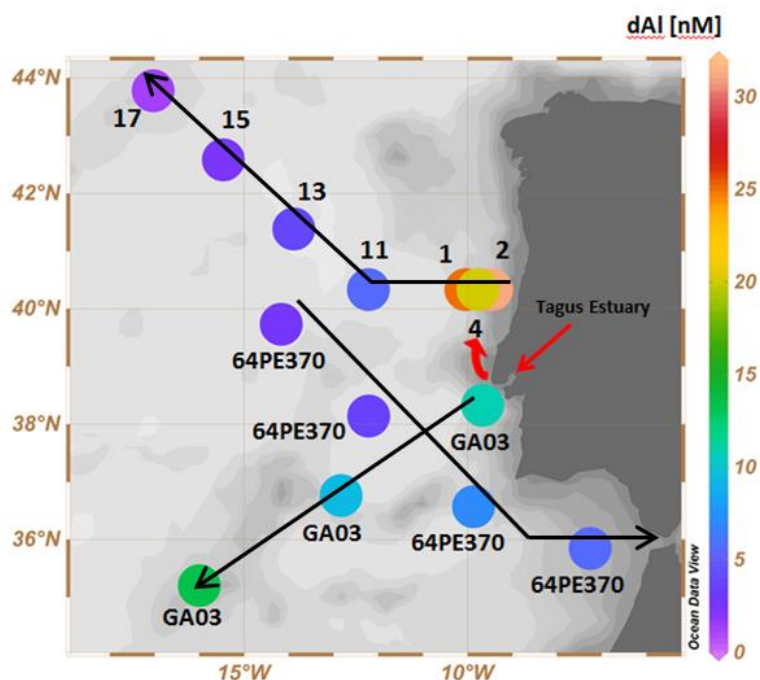
Figure 3: Surface concentration of dAl in the Iberian basin during GEOVIDE. GA03 refers to GEOTRACES section GA03 (Measures et al., 2015). 64PE370 refers to GEOTRACES section 64PE370 (Rolison et al., 2015). Black arrows show the cruise tracks. Red arrows show the location of the Tagus estuary and the northward direction of the Tagus plume. Plot created in Ocean Data View (Schlitzer, 2017)
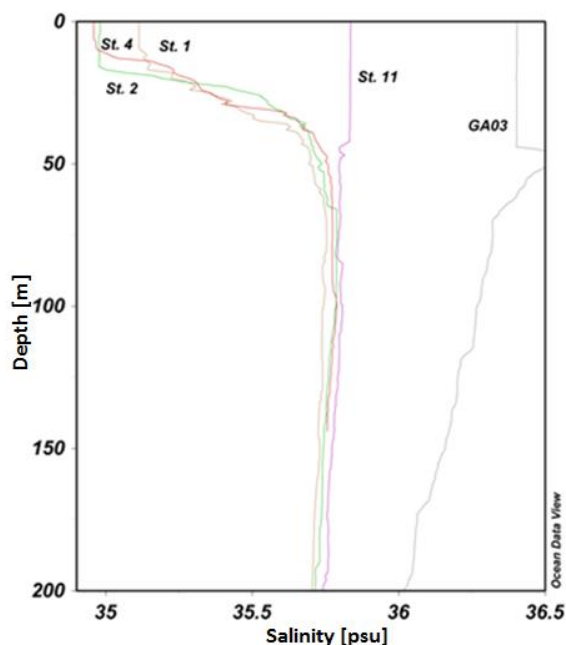
Figure 4: Salinity profiles showing an influence of fresh water for stations 1, 2 and 4. Profile labelled GA03 (Measures et al., 2015) shows the salinity profile for the closest station to the Tagus estuary (see Fig. 3 in the manuscript). Plot created in Ocean Data View (Schlitzer, 2017).

5   a)
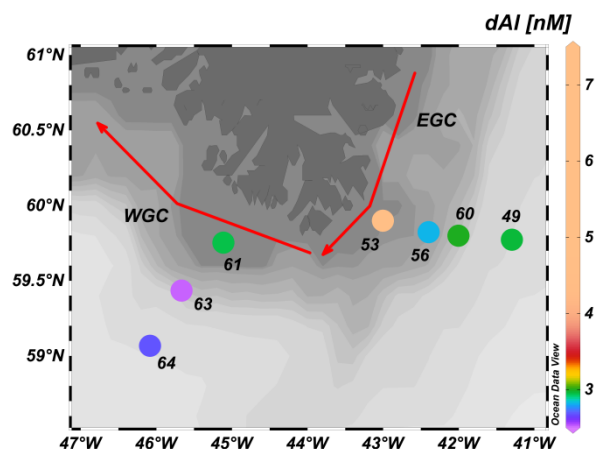
b)
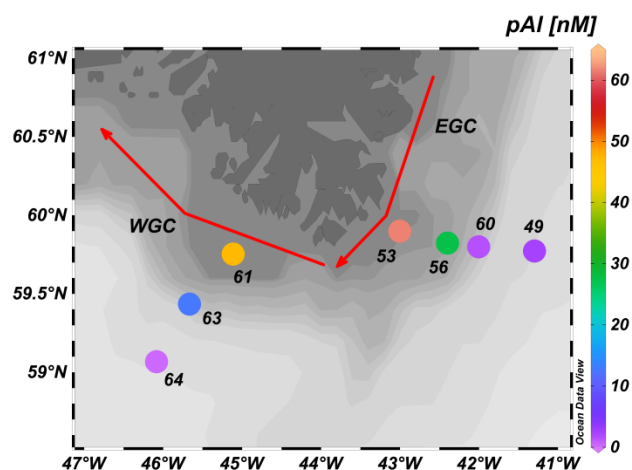
c)
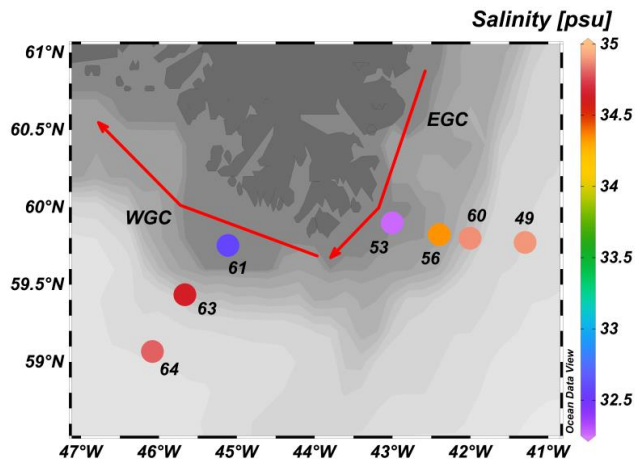
Figure 5: a) Surface concentration of dAl [nM] around SE and SW Greenland. b) Surface concentration of pAl [nM] (Gourain et al., 2017) around SE and SW Greenland. c) Salinity [psu] around SE and SW Greenland. Red arrows represent the main surface currents. EGC and WGC stand for East Greenland Current and West Greenland Current respectively. Plot created in Ocean Data View (Schlitzer, 2017).

Table 1: Correlations between salinity (S) and dAl and pAl for the eastern and western transects off Greenland. Endmember salinity 0 estimations for dAl and pAl.

Transect	Correlation S vs dAl	R^2	Correlation S vs pAl	R^2	Endmember S=0 dAl – pAl [nM]
Eastern flank	dAl = -1.6586 S + 60.527	0.94	pAl = - 22.018 S+773.7	0.95	60.5 - 773.7
Western flank	dAl = -0.1013 S + 6.24	0.89	pAl = -19.272 S+675.11	0.97	6.24 - 675.11

a)

b)
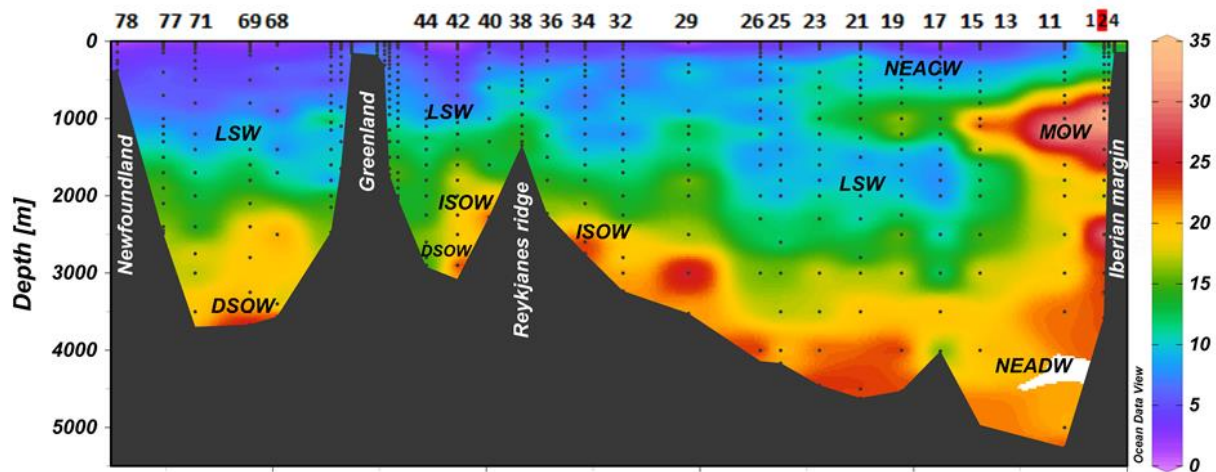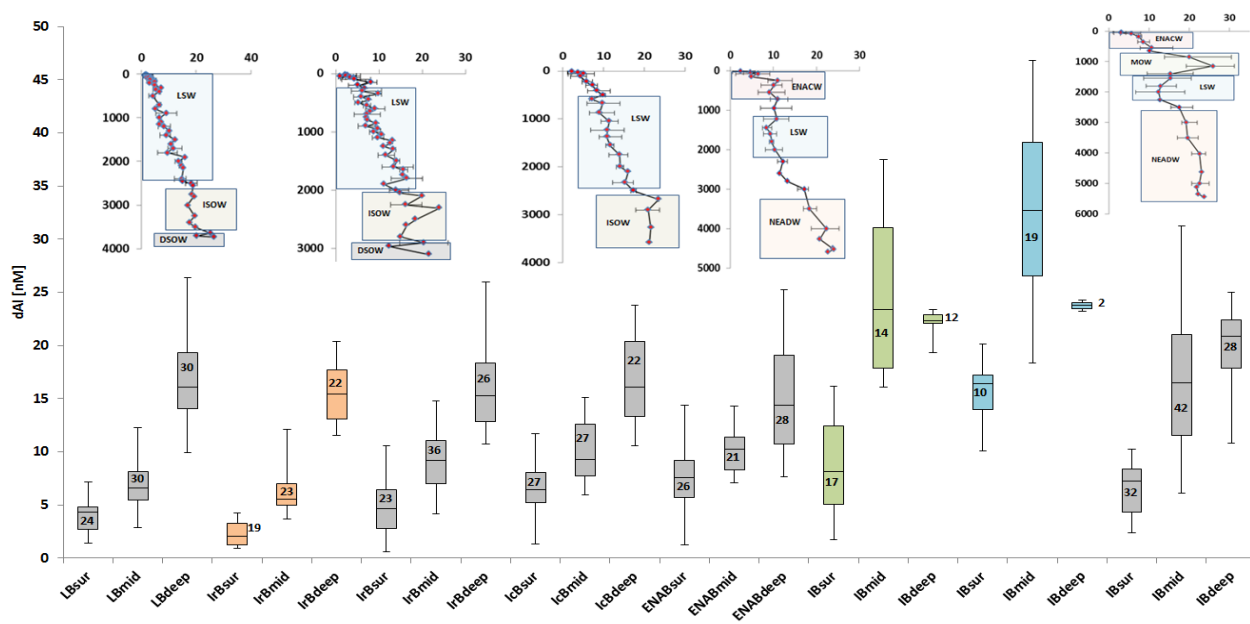
c)
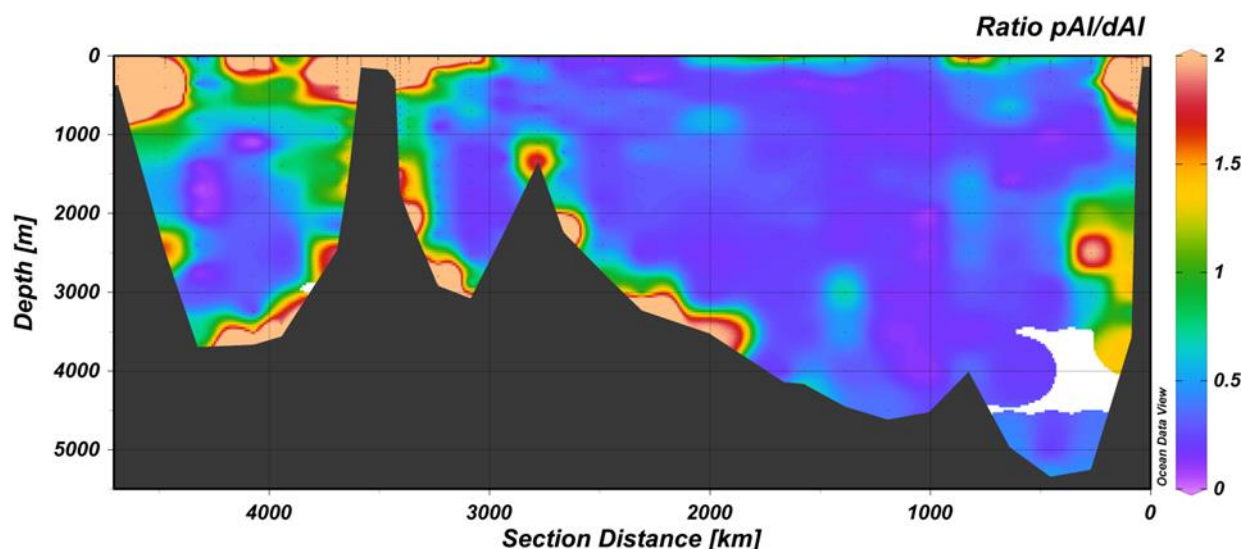
Figure 6: a) Cross-section plot of dAl concentrations [nM] over the full depth of the water column. Numbers represent the station numbers. On the Greenland shelf, stations numbers are as follow: From right to left 49, 60, 56, 53, 61, 63 and 64. Discrete sampling depths are indicated by filled black dots. For reference to water masses please refer to figure 1 b. b) Average dAl depth (x axis is [dAl] in nM and y axis is depth in m) profiles (see section 3.1 for stations) and Box-Whiskers plots for the different basins relative to depth. Sur: 50-500 m; Mid: 500-2500; Deep: 2500-seafloor. Numbers represent number of observations. Note that for the IrB and LB sur, mid and deep stand for 50-300, 300-1500 and 1500-seafloor as these basins are less deep. Blue, green and orange boxes are data from GEOTRACES cruise GA03 (Measures et al., 2015), 64PE370 (Rolison et al., 2015) and GA02 (Middag et al., 2015b), respectively. c) Cross-section plot of the pAl to dAl ratio (mol :mol) over the full depth of the water column. Plot created in Ocean Data View (Schlitzer, 2017).
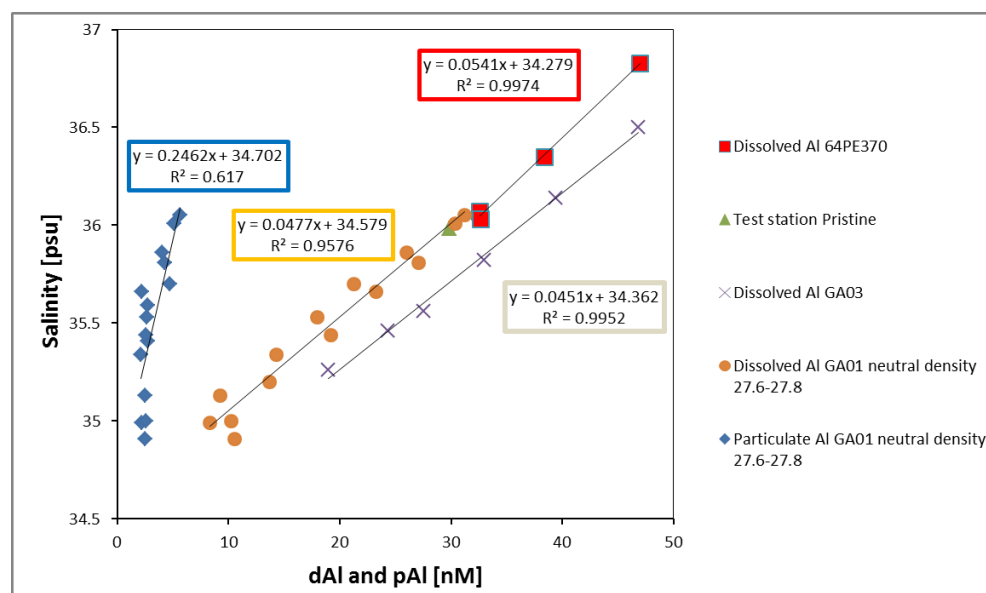
Figure 7: Dissolved Al and particulate Al (pAl) (Gourain et al., this issue) concentrations against salinity for the Mediterranean Outflow Water (MOW) between the neutral density layer 27.6 and 27.8 kg m^{-3}. GA03 (Measures et al., 2015), 64PE370 (Rolison et al., 2015) and test station Pristine (Rijkenberg et al., 2015).
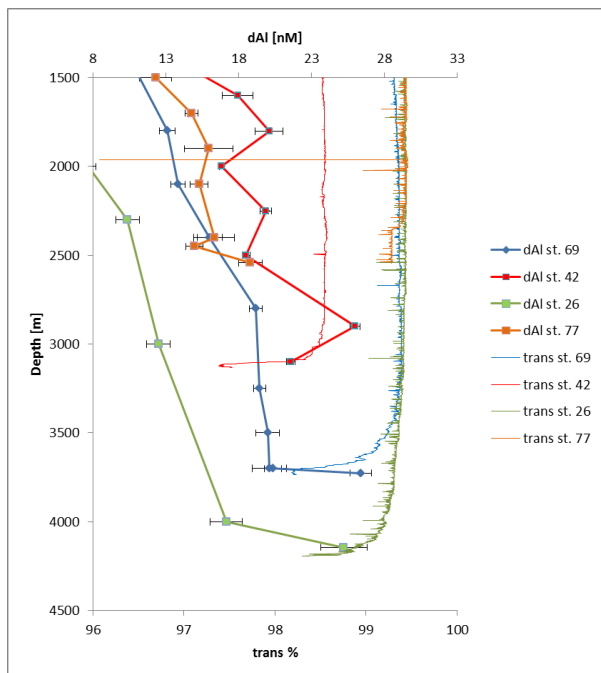
Figure 8: Dissolved Al [nM] and beam transmissometer [%] profiles for stations 26, 42, 69 and 77.